Search for Lepton Flavor Violation in the Decay $\tau^{\pm} \to \mu^{\pm}\gamma$

B. Aubert,[1] R. Barate,[1] D. Boutigny,[1] F. Couderc,[1] Y. Karyotakis,[1] J. P. Lees,[1] V. Poireau,[1] V. Tisserand,[1] A. Zghiche,[1]
E. Grauges-Pous,[2] A. Palano,[3] A. Pompili,[3] J. C. Chen,[4] N. D. Qi,[4] G. Rong,[4] P. Wang,[4] Y. S. Zhu,[4] G. Eigen,[5] I. Ofte,[5]
B. Stugu,[5] G. S. Abrams,[6] A. W. Borgland,[6] A. B. Breon,[6] D. N. Brown,[6] J. Button-Shafer,[6] R. N. Cahn,[6] E. Charles,[6]
C. T. Day,[6] M. S. Gill,[6] A. V. Gritsan,[6] Y. Groysman,[6] R. G. Jacobsen,[6] R. W. Kadel,[6] J. Kadyk,[6] L. T. Kerth,[6]
Yu. G. Kolomensky,[6] G. Kukartsev,[6] G. Lynch,[6] L. M. Mir,[6] P. J. Oddone,[6] T. J. Orimoto,[6] M. Pripstein,[6] N. A. Roe,[6]
M. T. Ronan,[6] W. A. Wenzel,[6] M. Barrett,[7] K. E. Ford,[7] T. J. Harrison,[7] A. J. Hart,[7] C. M. Hawkes,[7] S. E. Morgan,[7]
A. T. Watson,[7] M. Fritsch,[8] K. Goetzen,[8] T. Held,[8] H. Koch,[8] B. Lewandowski,[8] M. Pelizaeus,[8] K. Peters,[8] T. Schroeder,[8]
M. Steinke,[8] J. T. Boyd,[9] J. P. Burke,[9] N. Chevalier,[9] W. N. Cottingham,[9] M. P. Kelly,[9] T. E. Latham,[9] F. F. Wilson,[9]
T. Cuhadar-Donszelmann,[10] C. Hearty,[10] N. S. Knecht,[10] T. S. Mattison,[10] J. A. McKenna,[10] D. Thiessen,[10] A. Khan,[11]
P. Kyberd,[11] L. Teodorescu,[11] A. E. Blinov,[12] V. E. Blinov,[12] V. P. Druzhinin,[12] V. B. Golubev,[12] V. N. Ivanchenko,[12]
E. A. Kravchenko,[12] A. P. Onuchin,[12] S. I. Serednyakov,[12] Yu. I. Skovpen,[12] E. P. Solodov,[12] A. N. Yushkov,[12] D. Best,[13]
M. Bruinsma,[13] M. Chao,[13] I. Eschrich,[13] D. Kirkby,[13] A. J. Lankford,[13] M. Mandelkern,[13] R. K. Mommsen,[13]
W. Roethel,[13] D. P. Stoker,[13] C. Buchanan,[14] B. L. Hartfiel,[14] A. J. R. Weinstein,[14] S. D. Foulkes,[15] J. W. Gary,[15] O. Long,[15]
B. C. Shen,[15] K. Wang,[15] D. del Re,[16] H. K. Hadavand,[16] E. J. Hill,[16] D. B. MacFarlane,[16] H. P. Paar,[16] Sh. Rahatlou,[16]
V. Sharma,[16] J. W. Berryhill,[17] C. Campagnari,[17] A. Cunha,[17] B. Dahmes,[17] T. M. Hong,[17] A. Lu,[17] M. A. Mazur,[17]
J. D. Richman,[17] W. Verkerke,[17] T. W. Beck,[18] A. M. Eisner,[18] C. J. Flacco,[18] C. A. Heusch,[18] J. Kroseberg,[18]
W. S. Lockman,[18] G. Nesom,[18] T. Schalk,[18] B. A. Schumm,[18] A. Seiden,[18] P. Spradlin,[18] D. C. Williams,[18] M. G. Wilson,[18]
J. Albert,[19] E. Chen,[19] G. P. Dubois-Felsmann,[19] A. Dvoretskii,[19] D. G. Hitlin,[19] I. Narsky,[19] T. Piatenko,[19] F. C. Porter,[19]
A. Ryd,[19] A. Samuel,[19] S. Yang,[19] S. Jayatilleke,[20] G. Mancinelli,[20] B. T. Meadows,[20] M. D. Sokoloff,[20] F. Blanc,[21]
P. Bloom,[21] S. Chen,[21] W. T. Ford,[21] U. Nauenberg,[21] A. Olivas,[21] P. Rankin,[21] W. O. Ruddick,[21] J. G. Smith,[21]
K. A. Ulmer,[21] J. Zhang,[21] L. Zhang,[21] A. Chen,[22] E. A. Eckhart,[22] J. L. Harton,[22] A. Soffer,[22] W. H. Toki,[22] R. J. Wilson,[22]
Q. Zeng,[22] B. Spaan,[23] D. Altenburg,[24] T. Brandt,[24] J. Brose,[24] M. Dickopp,[24] E. Feltresi,[24] A. Hauke,[24] H. M. Lacker,[24]
E. Maly,[24] R. Nogowski,[24] S. Otto,[24] A. Petzold,[24] G. Schott,[24] J. Schubert,[24] K. R. Schubert,[24] R. Schwierz,[24]
J. E. Sundermann,[24] D. Bernard,[25] G. R. Bonneaud,[25] P. Grenier,[25] S. Schrenk,[25] Ch. Thiebaux,[25] G. Vasileiadis,[25]
M. Verderi,[25] D. J. Bard,[26] P. J. Clark,[26] F. Muheim,[26] S. Playfer,[26] Y. Xie,[26] M. Andreotti,[27] V. Azzolini,[27] D. Bettoni,[27]
C. Bozzi,[27] R. Calabrese,[27] G. Cibinetto,[27] E. Luppi,[27] M. Negrini,[27] L. Piemontese,[27] A. Sarti,[27] F. Anulli,[28]
R. Baldini-Ferroli,[28] A. Calcaterra,[28] R. de Sangro,[28] G. Finocchiaro,[28] P. Patteri,[28] I. M. Peruzzi,[28] M. Piccolo,[28]
A. Zallo,[28] A. Buzzo,[29] R. Capra,[29] R. Contri,[29] G. Crosetti,[29] M. Lo Vetere,[29] M. Macri,[29] M. R. Monge,[29] S. Passaggio,[29]
C. Patrignani,[29] E. Robutti,[29] A. Santroni,[29] S. Tosi,[29] S. Bailey,[30] G. Brandenburg,[30] K. S. Chaisanguanthum,[30]
M. Morii,[30] E. Won,[30] R. S. Dubitzky,[31] U. Langenegger,[31] J. Marks,[31] U. Uwer,[31] W. Bhimji,[32] D. A. Bowerman,[32]
P. D. Dauncey,[32] U. Egede,[32] J. R. Gaillard,[32] G. W. Morton,[32] J. A. Nash,[32] M. B. Nikolich,[32] G. P. Taylor,[32]
M. J. Charles,[33] G. J. Grenier,[33] U. Mallik,[33] A. K. Mohapatra,[33] J. Cochran,[34] H. B. Crawley,[34] J. Lamsa,[34] W. T. Meyer,[34]
S. Prell,[34] E. I. Rosenberg,[34] A. E. Rubin,[34] J. Yi,[34] N. Arnaud,[35] M. Davier,[35] X. Giroux,[35] G. Grosdidier,[35] A. Höcker,[35]
F. Le Diberder,[35] V. Lepeltier,[35] A. M. Lutz,[35] T. C. Petersen,[35] M. Pierini,[35] S. Plaszczynski,[35] M. H. Schune,[35]
G. Wormser,[35] C. H. Cheng,[36] D. J. Lange,[36] M. C. Simani,[36] D. M. Wright,[36] A. J. Bevan,[37] C. A. Chavez,[37]
J. P. Coleman,[37] I. J. Forster,[37] J. R. Fry,[37] E. Gabathuler,[37] R. Gamet,[37] D. E. Hutchcroft,[37] R. J. Parry,[37] D. J. Payne,[37]
C. Touramanis,[37] C. M. Cormack,[38] F. Di Lodovico,[38] C. L. Brown,[39] G. Cowan,[39] R. L. Flack,[39] H. U. Flaecher,[39]
M. G. Green,[39] P. S. Jackson,[39] T. R. McMahon,[39] S. Ricciardi,[39] F. Salvatore,[39] M. A. Winter,[39] D. Brown,[40] C. L. Davis,[40]
J. Allison,[41] N. R. Barlow,[41] R. J. Barlow,[41] M. C. Hodgkinson,[41] G. D. Lafferty,[41] M. T. Naisbit,[41] J. C. Williams,[41]
C. Chen,[42] A. Farbin,[42] W. D. Hulsbergen,[42] A. Jawahery,[42] D. Kovalskyi,[42] C. K. Lae,[42] V. Lillard,[42] D. A. Roberts,[42]
G. Blaylock,[43] C. Dallapiccola,[43] S. S. Hertzbach,[43] R. Kofler,[43] V. B. Koptchev,[43] T. B. Moore,[43] S. Saremi,[43]
H. Staengle,[43] S. Willocq,[43] R. Cowan,[44] K. Koeneke,[44] G. Sciolla,[44] S. J. Sekula,[44] F. Taylor,[44] R. K. Yamamoto,[44]
P. M. Patel,[45] S. H. Robertson,[45] A. Lazzaro,[46] V. Lombardo,[46] F. Palombo,[46] J. M. Bauer,[47] L. Cremaldi,[47]
V. Eschenburg,[47] R. Godang,[47] R. Kroeger,[47] J. Reidy,[47] D. A. Sanders,[47] D. J. Summers,[47] H. W. Zhao,[47] S. Brunet,[48]
D. Côté,[48] P. Taras,[48] H. Nicholson,[49] N. Cavallo,[50,*] F. Fabozzi,[50,*] C. Gatto,[50] L. Lista,[50] D. Monorchio,[50] P. Paolucci,[50]
D. Piccolo,[50] C. Sciacca,[50] M. Baak,[51] H. Bulten,[51] G. Raven,[51] H. L. Snoek,[51] L. Wilden,[51] C. P. Jessop,[52]
J. M. LoSecco,[52] T. Allmendinger,[53] G. Benelli,[53] K. K. Gan,[53] K. Honscheid,[53] D. Hufnagel,[53] H. Kagan,[53] R. Kass,[53]
T. Pulliam,[53] A. M. Rahimi,[53] R. Ter-Antonyan,[53] Q. K. Wong,[53] J. Brau,[54] R. Frey,[54] O. Igonkina,[54] M. Lu,[54]

C. T. Potter,[54] N. B. Sinev,[54] D. Strom,[54] E. Torrence,[54] F. Colecchia,[55] A. Dorigo,[55] F. Galeazzi,[55] M. Margoni,[55]
M. Morandin,[55] M. Posocco,[55] M. Rotondo,[55] F. Simonetto,[55] R. Stroili,[55] C. Voci,[55] M. Benayoun,[56] H. Briand,[56]
J. Chauveau,[56] P. David,[56] L. Del Buono,[56] Ch. de la Vaissière,[56] O. Hamon,[56] M. J. J. John,[56] Ph. Leruste,[56] J. Malclès,[56]
J. Ocariz,[56] L. Roos,[56] G. Therin,[56] P. K. Behera,[57] L. Gladney,[57] Q. H. Guo,[57] J. Panetta,[57] M. Biasini,[58] R. Covarelli,[58]
M. Pioppi,[58] C. Angelini,[59] G. Batignani,[59] S. Bettarini,[59] M. Bondioli,[59] F. Bucci,[59] G. Calderini,[59] M. Carpinelli,[59]
F. Forti,[59] M. A. Giorgi,[59] A. Lusiani,[59] G. Marchiori,[59] M. Morganti,[59] N. Neri,[59] E. Paoloni,[59] M. Rama,[59] G. Rizzo,[59]
G. Simi,[59] J. Walsh,[59] M. Haire,[60] D. Judd,[60] K. Paick,[60] D. E. Wagoner,[60] N. Danielson,[61] P. Elmer,[61] Y. P. Lau,[61] C. Lu,[61]
V. Miftakov,[61] J. Olsen,[61] A. J. S. Smith,[61] A. V. Telnov,[61] F. Bellini,[62] G. Cavoto,[61,62] A. D'Orazio,[62] E. Di Marco,[62]
R. Faccini,[62] F. Ferrarotto,[62] F. Ferroni,[62] M. Gaspero,[62] L. Li Gioi,[62] M. A. Mazzoni,[62] S. Morganti,[62] G. Piredda,[62]
F. Polci,[62] F. Safai Tehrani,[62] C. Voena,[62] S. Christ,[63] H. Schröder,[63] G. Wagner,[63] R. Waldi,[63] T. Adye,[64] N. De Groot,[64]
B. Franek,[64] G. P. Gopal,[64] E. O. Olaiya,[64] R. Aleksan,[65] S. Emery,[65] A. Gaidot,[65] S. F. Ganzhur,[65] P.-F. Giraud,[65]
G. Graziani,[65] G. Hamel de Monchenault,[65] W. Kozanecki,[65] M. Legendre,[65] G. W. London,[65] B. Mayer,[65] G. Vasseur,[65]
Ch. Yèche,[65] M. Zito,[65] M. V. Purohit,[66] A. W. Weidemann,[66] J. R. Wilson,[66] F. X. Yumiceva,[66] T. Abe,[67] D. Aston,[67]
R. Bartoldus,[67] N. Berger,[67] A. M. Boyarski,[67] O. L. Buchmueller,[67] R. Claus,[67] M. R. Convery,[67] M. Cristinziani,[67]
G. De Nardo,[67] J. C. Dingfelder,[67] D. Dong,[67] J. Dorfan,[67] D. Dujmic,[67] W. Dunwoodie,[67] S. Fan,[67] R. C. Field,[67]
T. Glanzman,[67] S. J. Gowdy,[67] T. Hadig,[67] V. Halyo,[67] C. Hast,[67] T. Hryn'ova,[67] W. R. Innes,[67] M. H. Kelsey,[67] P. Kim,[67]
M. L. Kocian,[67] D. W. G. S. Leith,[67] J. Libby,[67] S. Luitz,[67] V. Luth,[67] H. L. Lynch,[67] H. Marsiske,[67] R. Messner,[67]
D. R. Muller,[67] C. P. O'Grady,[67] V. E. Ozcan,[67] A. Perazzo,[67] M. Perl,[67] B. N. Ratcliff,[67] A. Roodman,[67] A. A. Salnikov,[67]
R. H. Schindler,[67] J. Schwiening,[67] A. Snyder,[67] A. Soha,[67] J. Stelzer,[67] J. Strube,[54,67] D. Su,[67] M. K. Sullivan,[67]
J. Va'vra,[67] S. R. Wagner,[67] M. Weaver,[67] W. J. Wisniewski,[67] M. Wittgen,[67] D. H. Wright,[67] A. K. Yarritu,[67]
C. C. Young,[67] P. R. Burchat,[68] A. J. Edwards,[68] S. A. Majewski,[68] B. A. Petersen,[68] C. Roat,[68] M. Ahmed,[69] S. Ahmed,[69]
M. S. Alam,[69] J. A. Ernst,[69] M. A. Saeed,[69] M. Saleem,[69] F. R. Wappler,[69] W. Bugg,[70] M. Krishnamurthy,[70]
S. M. Spanier,[70] R. Eckmann,[71] H. Kim,[71] J. L. Ritchie,[71] A. Satpathy,[71] R. F. Schwitters,[71] J. M. Izen,[72] I. Kitayama,[72]
X. C. Lou,[72] S. Ye,[72] F. Bianchi,[73] M. Bona,[73] F. Gallo,[73] D. Gamba,[73] L. Bosisio,[74] C. Cartaro,[74] F. Cossutti,[74]
G. Della Ricca,[74] S. Dittongo,[74] S. Grancagnolo,[74] L. Lanceri,[74] P. Poropat,[74,†] L. Vitale,[74] G. Vuagnin,[74]
F. Martinez-Vidal,[2,75] R. S. Panvini,[76,†] Sw. Banerjee,[77] B. Bhuyan,[77] C. M. Brown,[77] D. Fortin,[77] K. Hamano,[77]
P. D. Jackson,[77] R. Kowalewski,[77] J. M. Roney,[77] R. J. Sobie,[77] Z. Yun,[77] J. J. Back,[78] P. F. Harrison,[78] G. B. Mohanty,[78]
H. R. Band,[79] X. Chen,[79] B. Cheng,[79] S. Dasu,[79] M. Datta,[79] A. M. Eichenbaum,[79] K. T. Flood,[79] M. Graham,[79]
J. J. Hollar,[79] J. R. Johnson,[79] P. E. Kutter,[79] H. Li,[79] R. Liu,[79] A. Mihalyi,[79] Y. Pan,[79] R. Prepost,[79] P. Tan,[79]
J. H. von Wimmersperg-Toeller,[79] J. Wu,[79] S. L. Wu,[79] Z. Yu,[79] M. G. Greene,[80] and H. Neal[80]

(*BABAR* Collaboration)

[1]*Laboratoire de Physique des Particules, F-74941 Annecy-le-Vieux, France*
[2]*IFAE, Universitat Autonoma de Barcelona, E-08193 Bellaterra, Barcelona, Spain*
[3]*Università di Bari, Dipartimento di Fisica and INFN, I-70126 Bari, Italy*
[4]*Institute of High Energy Physics, Beijing 100039, China*
[5]*University of Bergen, Institute of Physics, N-5007 Bergen, Norway*
[6]*Lawrence Berkeley National Laboratory and University of California, Berkeley, California 94720, USA*
[7]*University of Birmingham, Birmingham B15 2TT, United Kingdom*
[8]*Ruhr Universität Bochum, Institut für Experimentalphysik 1, D-44780 Bochum, Germany*
[9]*University of Bristol, Bristol BS8 1TL, United Kingdom*
[10]*University of British Columbia, Vancouver, British Columbia, Canada V6T 1Z1*
[11]*Brunel University, Uxbridge, Middlesex UB8 3PH, United Kingdom*
[12]*Budker Institute of Nuclear Physics, Novosibirsk 630090, Russia*
[13]*University of California at Irvine, Irvine, California 92697, USA*
[14]*University of California at Los Angeles, Los Angeles, California 90024, USA*
[15]*University of California at Riverside, Riverside, California 92521, USA*
[16]*University of California at San Diego, La Jolla, California 92093, USA*
[17]*University of California at Santa Barbara, Santa Barbara, California 93106, USA*
[18]*University of California at Santa Cruz, Institute for Particle Physics, Santa Cruz, California 95064, USA*
[19]*California Institute of Technology, Pasadena, California 91125, USA*
[20]*University of Cincinnati, Cincinnati, Ohio 45221, USA*
[21]*University of Colorado, Boulder, Colorado 80309, USA*
[22]*Colorado State University, Fort Collins, Colorado 80523, USA*

[23]Universität Dortmund, Institut fur Physik, D-44221 Dortmund, Germany

[24]Technische Universität Dresden, Institut für Kern- und Teilchenphysik, D-01062 Dresden, Germany

[25]Ecole Polytechnique, LLR, F-91128 Palaiseau, France

[26]University of Edinburgh, Edinburgh EH9 3JZ, United Kingdom

[27]Università di Ferrara, Dipartimento di Fisica and INFN, I-44100 Ferrara, Italy

[28]Laboratori Nazionali di Frascati dell'INFN, I-00044 Frascati, Italy

[29]Università di Genova, Dipartimento di Fisica and INFN, I-16146 Genova, Italy

[30]Harvard University, Cambridge, Massachusetts 02138, USA

[31]Universität Heidelberg, Physikalisches Institut, Philosophenweg 12, D-69120 Heidelberg, Germany

[32]Imperial College London, London SW7 2AZ, United Kingdom

[33]University of Iowa, Iowa City, Iowa 52242, USA

[34]Iowa State University, Ames, Iowa 50011-3160, USA

[35]Laboratoire de l'Accélérateur Linéaire, F-91898 Orsay, France

[36]Lawrence Livermore National Laboratory, Livermore, California 94550, USA

[37]University of Liverpool, Liverpool L69 72E, United Kingdom

[38]Queen Mary, University of London, London E1 4NS, United Kingdom

[39]University of London, Royal Holloway and Bedford New College, Egham, Surrey TW20 0EX, United Kingdom

[40]University of Louisville, Louisville, Kentucky 40292, USA

[41]University of Manchester, Manchester M13 9PL, United Kingdom

[42]University of Maryland, College Park, Maryland 20742, USA

[43]University of Massachusetts, Amherst, Massachusetts 01003, USA

[44]Massachusetts Institute of Technology, Laboratory for Nuclear Science, Cambridge, Massachusetts 02139, USA

[45]McGill University, Montréal, Québec, Canada H3A 2T8

[46]Università di Milano, Dipartimento di Fisica and INFN, I-20133 Milano, Italy

[47]University of Mississippi, University, Mississippi 38677, USA

[48]Université de Montréal, Laboratoire René J. A. Lévesque, Montréal, Québec, Canada H3C 3J7

[49]Mount Holyoke College, South Hadley, Massachusetts 01075, USA

[50]Università di Napoli Federico II, Dipartimento di Scienze Fisiche and INFN, I-80126, Napoli, Italy

[51]NIKHEF, National Institute for Nuclear Physics and High Energy Physics, NL-1009 DB Amsterdam, The Netherlands

[52]University of Notre Dame, Notre Dame, Indiana 46556, USA

[53]The Ohio State University, Columbus, Ohio 43210, USA

[54]University of Oregon, Eugene, Oregon 97403, USA

[55]Università di Padova, Dipartimento di Fisica and INFN, I-35131 Padova, Italy

[56]Universités Paris VI et VII, Laboratoire de Physique Nucléaire et de Hautes Energies, F-75252 Paris, France

[57]University of Pennsylvania, Philadelphia, Pennsylvania 19104, USA

[58]Università di Perugia, Dipartimento di Fisica and INFN, I-06100 Perugia, Italy

[59]Università di Pisa, Dipartimento di Fisica, Scuola Normale Superiore and INFN, I-56127 Pisa, Italy

[60]Prairie View A&M University, Prairie View, Texas 77446, USA

[61]Princeton University, Princeton, New Jersey 08544, USA

[62]Università di Roma La Sapienza, Dipartimento di Fisica and INFN, I-00185 Roma, Italy

[63]Universität Rostock, D-18051 Rostock, Germany

[64]Rutherford Appleton Laboratory, Chilton, Didcot, Oxon OX11 0QX, United Kingdom

[65]DSM/Dapnia, CEA/Saclay, F-91191 Gif-sur-Yvette, France

[66]University of South Carolina, Columbia, South Carolina 29208, USA

[67]Stanford Linear Accelerator Center, Stanford, California 94309, USA

[68]Stanford University, Stanford, California 94305-4060, USA

[69]State University of New York, Albany, New York 12222, USA

[70]University of Tennessee, Knoxville, Tennessee 37996, USA

[71]University of Texas at Austin, Austin, Texas 78712, USA

[72]University of Texas at Dallas, Richardson, Texas 75083, USA

[73]Università di Torino, Dipartimento di Fisica Sperimentale and INFN, I-10125 Torino, Italy

[74]Università di Trieste, Dipartimento di Fisica and INFN, I-34127 Trieste, Italy

[75]IFIC, Universitat de Valencia-CSIC, E-46071 Valencia, Spain

[76]Vanderbilt University, Nashville, Tennessee 37235, USA

[77]University of Victoria, Victoria, British Columbia, Canada V8W 3P6

[78]Department of Physics, University of Warwick, Coventry CV4 7AL, United Kingdom

[79]University of Wisconsin, Madison, Wisconsin 53706, USA

[80]Yale University, New Haven, Connecticut 06511, USA

A search for the nonconservation of lepton flavor number in the decay $\tau^{\pm} \to \mu^{\pm}\gamma$ has been performed using 2.07×10^8 $e^+e^- \to \tau^+\tau^-$ events produced at a center-of-mass energy near 10.58 GeV with the *BABAR* detector at the PEP-II storage ring. We find no evidence for a signal and set an upper limit on the branching ratio of $\mathcal{B}(\tau^{\pm} \to \mu^{\pm}\gamma) < 6.8 \times 10^{-8}$ at 90% confidence level.

Decays violating the lepton flavor number, if observed, would be among the most theoretically clean signatures of new physics, and the decay $\tau^{\pm} \to \mu^{\pm}\gamma$ is one such process. It is expected with rates as high as several parts per million in some supersymmetric models [1,2], despite the stringent experimental limit on the related $\mu^{\pm} \to e^{\pm}\gamma$ decay [3]. In a modest extension to the standard model (SM) incorporating finite ν masses [4], the branching ratio is many orders of magnitude below experimental accessibility [5], and so an observation of this mode would unambiguously indicate new physics. Currently the most stringent limit is $\mathcal{B}(\tau^{\pm} \to \mu^{\pm}\gamma) < 3.1 \times 10^{-7}$ at 90% confidence level (C.L.) from the BELLE experiment [6].

The search for $\tau^{\pm} \to \mu^{\pm}\gamma$ decays reported here uses data recorded by the *BABAR* detector at the SLAC PEP-II asymmetric-energy e^+e^- storage ring. The data sample consists of an integrated luminosity of $\mathcal{L} = 210.6$ fb^{-1} recorded at a center-of-mass energy ($\sqrt{s}$) of $\sqrt{s} = 10.58$ GeV and 21.6 fb^{-1} recorded at $\sqrt{s} = 10.54$ GeV. The luminosity-weighted average cross section for $e^+e^- \to \tau^+\tau^-$ is $\sigma_{\tau\tau} = (0.89 \pm 0.02)$ nb [7], corresponding to a data sample of 2.07×10^8 τ-pair events.

The *BABAR* detector is described in detail in Ref. [8]. Charged particles are reconstructed as tracks with a 5-layer silicon vertex tracker and a 40-layer drift chamber (DCH) inside a 1.5 T solenoidal magnet. An electromagnetic calorimeter (EMC) consisting of 6580 CsI(Tl) crystals is used to identify electrons and photons. The flux return of the solenoid, instrumented with resistive plate chambers (IFR), is used to identify muons.

The signature of the signal process is the presence of an isolated μ and γ having an invariant mass consistent with that of the τ (1.777 GeV/c^2 [9]) and a total energy ($E_{\mu\gamma}$) equal to $\sqrt{s}/2$ in the event center-of-mass (c.m.) frame, as well as properties of the other particles in the event that are consistent with a SM τ decay. Such events are simulated with higher-order radiative corrections using the KK2F Monte Carlo (MC) generator [7] where one τ decays into $\mu\gamma$ according to phase space [10], while the other τ decays according to measured rates [11] simulated with TAUOLA [12,13]. The detector response is simulated with GEANT4 [14]. The simulated events for signal as well as SM background processes [7,12,13,15,16] are then reconstructed in the same manner as data. The MC backgrounds are used for selection optimization and efficiency systematic studies, but not for the final background estimation, which relies solely on data.

Events with two or four well reconstructed tracks and zero net charge are selected. The magnitude of the thrust vector calculated with all observed charged and neutral particles, characterizing the direction of maximum energy flow in the event [17], is required to lie between 0.900 and 0.975 to suppress $e^+e^- \to q\bar{q}$ backgrounds with low thrust and $e^+e^- \to \mu^+\mu^-$ and Bhabha backgrounds with thrust close to unity. Other non-τ backgrounds are suppressed by requiring the polar angle (θ_{miss}) of the missing momentum associated with the neutrinos in the event to lie within the detector acceptance ($-0.76 < \cos\theta_{\text{miss}} < 0.92$), and the scaled missing c.m. transverse momentum relative to the beam axis ($p^T_{\text{miss}}/\sqrt{s}$) to be greater than 0.068 (0.009) for events with two (four) tracks.

The signal-side hemisphere, defined with respect to the thrust axis, is required to contain one track with c.m. momentum less than 4.5 GeV/c and at least one γ with a c.m. energy greater than 200 MeV. The track must be identified as a μ using DCH, EMC, and IFR information, and the γ candidate is the one that gives the mass of the $\mu\gamma$ system closest to the τ mass. This provides the correct pairing for 99.9% of selected signal events. The resolution of the $\mu\gamma$ mass is improved by assigning the point of closest approach of the μ track to the e^+e^- collision axis as the origin of the γ candidate and by using a kinematic fit with $E_{\mu\gamma}$ constrained to $\sqrt{s}/2$. This energy-constrained mass (m_{EC}) and $\Delta E = E_{\mu\gamma} - \sqrt{s}/2$ are independent variables apart from small correlations arising from initial and final state radiation. The mean and standard deviation of the m_{EC} and ΔE distributions for reconstructed MC signal events are $\langle m_{\text{EC}} \rangle = 1777$ MeV/c^2, $\sigma(m_{\text{EC}}) = 9$ MeV/c^2, $\langle \Delta E \rangle = -9$ MeV, and $\sigma(\Delta E) = 45$ MeV, where the shift in $\langle \Delta E \rangle$ comes from photon energy reconstruction effects. We blind the data events within a 3σ ellipse centered on $\langle m_{\text{EC}} \rangle$ and $\langle \Delta E \rangle$ until completing all optimization and systematic studies of the selection criteria.

The dominant backgrounds are from $e^+e^- \to \mu^+\mu^-$ and $e^+e^- \to \tau^+\tau^-$ (with a $\tau^{\pm} \to \mu^{\pm}\nu\bar{\nu}$ decay) events with an energetic γ from initial or final state radiation or in the τ decay. For these backgrounds, the γ is predominantly along the μ flight direction; thus we require $|\cos\theta_H| < 0.8$, where θ_H is the angle between the μ momentum in the reconstructed τ rest frame and the τ momentum in the laboratory frame. Backgrounds arising from $\tau^{\pm} \to h^{\pm}(\geq 1)\pi^0\nu$ decays with the hadronic track (h) misidentified as a μ are reduced by requiring the total c.m. energy of nonsignal γ candidates in the signal-side hemisphere to be less than 200 MeV. If the reconstructed neutral candidate identified as the signal γ has at least 1%

likelihood of arising from overlapping daughters in $\pi^0 \rightarrow \gamma\gamma$ decays, then the event is rejected.

The tag-side hemisphere, which is expected to contain a SM τ decay, is required to have a total invariant mass less than 1.6 GeV/c^2 and a c.m. momentum for each track less than 4.0 GeV/c to reduce background from $e^+e^- \rightarrow q\bar{q}$ and $e^+e^- \rightarrow \mu^+\mu^-$ processes, respectively. The $q\bar{q}$ background is further reduced by requiring the hemisphere to have no more than six γ candidates.

A tag-side hemisphere containing a single track is classified as e-tag, μ-tag, or h-tag if the total photon c.m. energy in the hemisphere is no more than 200 MeV and the track is exclusively identified as an electron (e-tag), as a muon (μ-tag), or as neither (h-tag). If the total photon c.m. energy in the hemisphere is more than 200 MeV, then events are selected if the track is exclusively identified as an electron ($e\gamma$-tag) or as neither an electron nor a muon
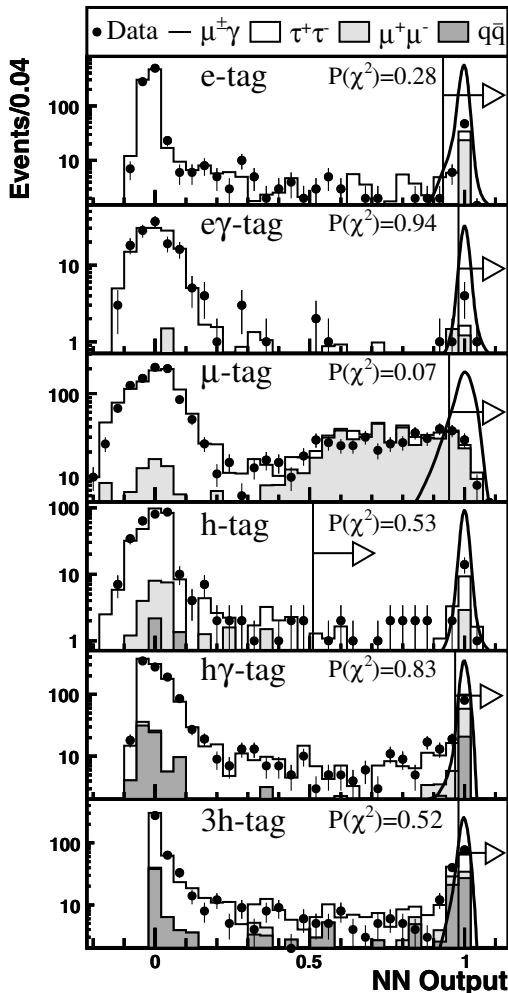

FIG. 1. NN output shown for data (dots), MC backgrounds (histograms normalized to the luminosity), and MC signal (curves with arbitrary normalization) in the GSB region. Lines with arrows indicate optimized cut positions. The probability of the data-MC χ^2 is indicated for each tag mode.

($h\gamma$-tag). These allow for the presence of radiation in $\tau^\pm \rightarrow e^\pm \nu\bar{\nu}$ decays and for photons from $\pi^0 \rightarrow \gamma\gamma$ in $\tau^\pm \rightarrow h^\pm (\geq 1)\pi^0\nu$ decays. If the tag side contains three tracks, the event is classified as a $3h$ tag. We explored other tag-side channels, but the sensitivity of the search does not improve by including them.

Hadronic τ decays have only one missing ν, a feature used to purify the sample. Taking the tag-side τ direction to be opposite the fitted signal $\mu\gamma$ candidate, we use all tracks and γ candidates on the tag side to calculate the invariant mass squared of the missing ν (m_ν^2) and require $|m_\nu^2|$ to be less than 0.4 GeV$^2/c^4$ for h-tag and $3h$-tag events and less than 0.8 GeV$^2/c^4$ for $h\gamma$-tag events.

At this stage of the analysis, 15% of the MC signal events survive within a grand sideband (GSB) region defined as $m_{\text{EC}} \in [1.5, 2.1]$ GeV/c^2, $\Delta E \in [-1.0, 0.5]$ GeV. The nonblinded part of the GSB contains 4688 data events, which agrees with the MC background expectation of 4924 events to within 5%. Out of these MC events, 80% are from $e^+e^- \rightarrow \tau^+\tau^-$, 82% of which are $\tau^\pm \rightarrow \mu^\pm \nu\bar{\nu}$ decays on the signal side.

To further suppress the backgrounds, separate neural net (NN)–based discriminators are used for each of the six tags. Five observables serve as input to the NN: the missing mass of the event, the highest c.m. momentum of the tag-side track(s), $\cos\theta_H$, p_{miss}^T, and m_ν^2. Each NN is trained using data in the nonblinded part of the GSB to describe the background and $\mu\gamma$ MC in the full GSB region to describe the signal. The NN output distributions of the data (Fig. 1) are in good agreement with MC backgrounds in both shape and absolute rates, as are the input observables. The MC signal within a 2σ ellipse in the m_{EC}-ΔE plane centered on $\langle m_{\text{EC}}\rangle$ and $\langle\Delta E\rangle$ and the MC background interpolated from m_{EC} sidebands ($|m_{\text{EC}} - \langle m_{\text{EC}}\rangle| > 3\sigma$ within the GSB and $|\Delta E - \langle\Delta E\rangle| < 3\sigma$) are then used to optimize the cut value on the NN output based on the expected 90% C.L. upper limit. The optimized NN cut values are restricted to be >0.5. Within the $\pm 3\sigma$ band in ΔE, the MC predicts that 66% of the selected background comes from $e^+e^- \rightarrow \mu^+\mu^-$, 27% from $e^+e^- \rightarrow \tau^+\tau^-$, and the rest from $e^+e^- \rightarrow q\bar{q}$ processes.

With the data unblinded, we find four events in the 2σ signal ellipse where we expect 6.2 ± 0.5 events, obtained from a linear interpolation of the data in the m_{EC} sidebands. Other polynomials up to at least fifth order predict the same level of background to within half a standard deviation. The agreement between observed data and background expectations across the different tagging modes are shown in Table I.

The relative systematic uncertainties on the trigger efficiency, tracking and photon reconstruction efficiencies, and particle identification are estimated to be 1.2%, 1.3%, 1.8%, and 1.2%, respectively. We obtain a measure of the systematic error of the efficiency due to simulation uncertainties of the NN input variables by fixing each input

TABLE I.   Number of events for data and MC backgrounds for the different tags in the full GSB; in the 2σ signal ellipse, the number of events selected in data and expected from the data sidebands; the number of data events selected inside the $\pm 2\sigma$ band in ΔE; and the respective efficiencies (ε).

Tag		e	$e\gamma$	μ	h	$h\gamma$	$3h$	All
GSB	Data	57	6	67	31	92	78	331
	MC	46.4	2.7	63.1	19.2	108.9	64.9	305
	$\varepsilon(\%)$	1.88	0.27	1.80	1.44	3.72	1.85	11.0
2σ signal ellipse	Selected	1	0	1	0	1	1	4
	Expected from data	1.1	0.1	1.9	0.5	1.8	0.9	6.2
		± 0.2	± 0.1	± 0.3	± 0.1	± 0.3	± 0.2	± 0.5
	$\varepsilon(\%)$	1.27	0.18	1.31	0.89	2.56	1.22	7.42
$\pm 2\sigma$ in ΔE	Data	20	0	51	9	41	20	141
	$\varepsilon(\%)$	1.62	0.23	1.63	1.13	3.22	1.53	9.35

variable to its average value one at a time, without retraining or changing the architecture of the NN, and recalculating the efficiency. This has the effect of removing each input variable completely from the NN selection and gives a 1.9% relative error on the signal efficiency. Adding these errors in quadrature gives 3.4%. As we use 1.2×10^6 MC signal events, the contribution to the error arising from signal MC statistics is negligible.

Alternatively, these (and other potential sources of systematic uncertainty not necessarily accounted for in the above procedure) can be collectively estimated from the detector modeling uncertainty obtained by comparing data to the MC backgrounds in the nonblinded part of the GSB, where the background and signal have similar properties apart from m_{EC} and ΔE. Data and MC background statistics as well as signal efficiencies (ε) are shown in Table I inside the full GSB. The agreement in the GSB between data and the background MC for each tag mode and their combination validates the ability of the MC to simulate these signal-like events. The statistical precision of this data-to-MC ratio is augmented by using the expanded range $m_{EC} \in [1.0, 2.5]$ GeV/c^2 to obtain a value of $1.052 \pm 0.056(\text{stat}) \pm 0.024(\text{norm})$ in the nonblinded part of the GSB. To be conservative, we quote the total 6.1% uncertainty on this ratio, which includes a 2.3% normalization error on the product $\mathcal{L}\sigma_{\tau\tau}$, as the relative systematic error on the ε in the GSB.

To obtain the branching ratio, we perform an extended unbinned maximum likelihood (EML) fit to the m_{EC} data distribution (Fig. 2) after all requirements but that on m_{EC} have been applied. Within this $\pm 2\sigma$ band in ΔE the efficiencies for the different tag modes are given in Table I for a total value of $\varepsilon = (9.4 \pm 0.6)\%$, where the systematic error here includes an additional contribution from the ΔE requirement. A linear parametrization describes the background, and a double Gaussian serves as the probability density function (PDF) of the signal. Uncertainties in the mean and resolution of m_{EC} are incorporated into the fit by convoluting the signal PDF with

another Gaussian with $\sigma = 4$ MeV/c^2 and by increasing the σ of the convoluted Gaussian by 1 MeV/c^2. The quoted limit is insensitive to these variations, however.

In the EML fit, the number of signal events is given by $2\mathcal{L}\sigma_{\tau\tau}\varepsilon\mathcal{B}(\tau^\pm \to \mu^\pm\gamma)$, and we fit for the branching ratio the number of background events and slope of the background. The systematic uncertainty on ε is incorporated into the likelihood by adding ε as a fourth fit parameter under the constraint that it follows a Gaussian spread about its measured value within the estimated errors. This yields the same upper limit as the fit without the constraint on ε to within the quoted number of significant figures. The fit gives $\mathcal{B}(\tau^\pm \to \mu^\pm\gamma) = (-5.6 ^{+8.3}_{-6.3}) \times 10^{-8}$, which corresponds to the $-2.2 ^{+3.2}_{-2.4}$ signal and 143 ± 12 background
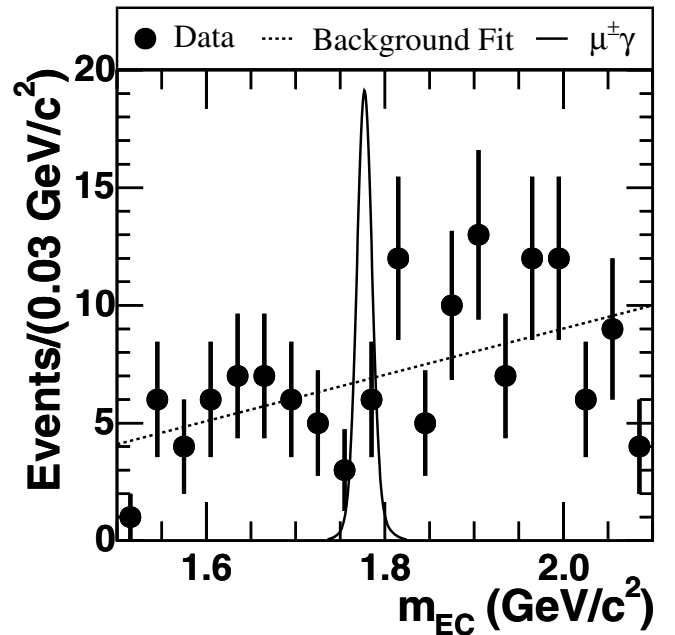

FIG. 2. m_{EC} distribution of data (dots), the background component of the fit (dotted line), and the MC signal (curve with arbitrary normalization) for $|\Delta E - \langle\Delta E\rangle| < 2\sigma$. The χ^2 between data and the background component is 16.0 for 20 bins.

events. From the likelihood function of this fit, a Bayesian upper limit can be derived [18].

In keeping with established $\tau^\pm \to \mu^\pm \gamma$ studies [6,19], we derive a frequentist upper limit [20]. We generate MC samples with Poisson-distributed numbers of signal and background events. The expected number of background events is fixed to 143, and we scan over the expected number of signal events, s. The m_{EC} values are distributed according to the signal and background PDFs, where the background slope is generated from a Gaussian distribution with mean and standard deviation given by the fit to the data. The number of signal events in each sample is extracted using the same EML fit procedure as that applied to the data. We vary s until we find a value for which 90% of the sample yields a fitted number of signal events greater than that observed in the data, i.e., -2.2. At 90% C.L. this procedure gives an upper limit of $\mathcal{B}(\tau^\pm \to \mu^\pm \gamma) < 6.8 \times 10^{-8}$ [21].

As confirmation of this result, we also undertake an analysis without the NN, having the same sensitivity of 12×10^{-8} for the expected 90% C.L. upper limit. Events with a tag-side muon are vetoed but single-track tag events are otherwise not classified. Cuts are applied on the signal μ momentum, signal γ energy, θ_{miss}, p^T_{miss}, the tag-side invariant mass, and ΔE, and m_{EC} is required to be within 30 MeV of m_τ. This selection retains 10.7% of the signal and has a background of 28.5 ± 2.3 events as estimated from the sidebands.

To enhance the signal to background discrimination, a likelihood ratio variable, $\mathcal{R}$, is built from four discriminating variables: p^T_{miss}, ΔE, the difference between the signal μ and γ energy in the c.m., and the acoplanarity between the signal $\mu\gamma$ system and the tag system. We observe no evidence of signal, and we compare the two-dimensional (m_{EC}, $\mathcal{R}$) distribution of the 27 events in data with the background and signal expectations, utilizing a classical frequentist CL_{S+B} method [22]. The limit set is consistent with the above value and amounts to a 90% C.L. limit of 9.4×10^{-8}.

---

*Also with Università della Basilicata, Potenza, Italy.
†Deceased.

[1] J. Hisano and D. Nomura, Phys. Rev. D **59**, 116005 (1999).

[2] S. F. King and M. Oliveira, Phys. Rev. D **60**, 035003 (1999).

[3] M. L. Brooks *et al.* (MEGA Collaboration), Phys. Rev. Lett. **83**, 1521 (1999). This currently provides the most stringent limit of $\mathcal{B}(\mu^\pm \to e^\pm \gamma) < 1.2 \times 10^{-11}$ at 90% C.L.

[4] Y. Fukuda *et al.* (Super-Kamiokande Collaboration), Phys. Rev. Lett. **81**, 1562 (1998); Q. R. Ahmad *et al.* (SNO Collaboration), Phys. Rev. Lett. **89**, 011301 (2002); M. H. Ahn *et al.* (K2K Collaboration), Phys. Rev. Lett. **90**, 041801 (2003); K. Eguchi *et al.* (KamLAND Collaboration), Phys. Rev. Lett. **90**, 021802 (2003).

[5] B. W. Lee and R. E. Shrock, Phys. Rev. D **16**, 1444 (1977). A value of $\Delta m^2_{32} \approx 3 \times 10^{-3}(eV/c^2)^2$ [4] and maximal mixing implies $\mathcal{B}(\tau^\pm \to \mu^\pm \gamma) \approx \mathcal{O}(10^{-54})$.

[6] K. Abe *et al.* (Belle Collaboration), Phys. Rev. Lett. **92**, 171802 (2004).

[7] B. F. Ward, S. Jadach, and Z. Was, Nucl. Phys. B (Proc. Suppl.) **116**, 73 (2003).

[8] B. Aubert *et al.* (*BABAR* Collaboration), Nucl. Instrum. Methods Phys. Res., Sect. A **479**, 1 (2002).

[9] J. Z. Bai *et al.* (BES Collaboration), Phys. Rev. D **53**, 20 (1996).

[10] Although the signal MC has been modeled using a phase space model, the limit obtained in this analysis is insensitive to this assumption as demonstrated by considering the two extreme cases of a $V - A$ and a $V + A$ form of interaction for the signal MC. The insensitivity is largely a consequence of the symmetric cut on $|\cos\theta_H|$.

[11] K. Hagiwara *et al.* (Particle Data Group), Phys. Rev. D **66**, 010001 (2002).

[12] S. Jadach, Z. Was, R. Decker, and J. H. Kuhn, Comput. Phys. Commun. **76**, 361 (1993).

[13] E. Barberio and Z. Was, Comput. Phys. Commun. **79**, 291 (1994).

[14] S. Agostinelli *et al.* (GEANT4 Collaboration), Nucl. Instrum. Methods Phys. Res., Sect. A **506**, 250 (2003).

[15] D. J. Lange, Nucl. Instrum. Methods Phys. Res., Sect. A **462**, 152 (2001).

[16] T. Sjöstrand, Comput. Phys. Commun. **82**, 74 (1994).

[17] S. Brandt *et al.*, Phys. Lett. **12**, 57 (1964); E. Farhi, Phys. Rev. Lett. **39**, 1587 (1977).

[18] A Bayesian upper limit assuming a uniform prior can be obtained by integrating the likelihood function of the fit, L, from zero to the value of the branching ratio that includes 90% of $\int_0^\infty L(\mathcal{B})d\mathcal{B}$. This gives a 90% C.L. upper limit of $\mathcal{B}(\tau^\pm \to \mu^\pm \gamma) < 14 \times 10^{-8}$. Integrating from $-\infty$ intead of zero changes this to 7.9×10^{-8}.

[19] S. Ahmed *et al.* (CLEO Collaboration), Phys. Rev. D **61**, 071101 (2000).

[20] I. Narsky, Nucl. Instrum. Methods Phys. Res., Sect. A **450**, 444 (2000). Subsequent to this publication, its author recommended employing a fit convention that allows for a negative yield.

[21] For an equivalent experiment with no signal, the probability of obtaining a 90% C.L. upper limit at or below 6.8×10^{-8} is 30%.

[22] T. Junk, Nucl. Instrum. Methods Phys. Res., Sect. A **434**, 435 (1999); A. L. Read, J. Phys. G **28**, 2693 (2002).